24th INTERNATIONAL CONGRESS ON SOUND AND VIBRATION
23–27 July 2017, London

ICSV24
23-27JULY 2017
LONDON CALLING

ON BRYAN'S LAW AND ANISOTROPIC NONLINEAR DAMPING

Stephan V. Joubert, Michael Y. Shatalov, Temple H. Fay and Getachew T. Sedebo
Tshwane University of Technology, Faculty of Science, Department of Mathematics and Statistics, South Africa
email: joubertsv@tut.ac.za

In 1890 G.H. Bryan discovered what we call Bryan's Law: "The vibration pattern of a revolving cylinder or bell revolves at a rate proportional to the inertial rotation rate of the cylinder or bell". We call the rotation rate of the vibration pattern the precession rate. A vibratory gyroscope (VG) operates using Bryan's factor (the proportionality constant mentioned in the law). It is known that linear anisotropic damping affects the precession rate of a perfectly manufactured VG rotating slowly about a symmetry axis, whereas neither linear nor nonlinear isotropic damping affect it. In this paper, using graphical evidence obtained from a numerical experiment, we observe that anisotropic quadratic damping apparently does appear to affect the precession rate of such VGs. The equations of motion given here indicate that the experiment may be extended to any order of or combination of nonlinear anisotropic damping with similar results. To achieve this we define a new generalised form of Rayleigh's dissipation function that allows the introduction of anisotropic nonlinear damping into the equations of motion of a perfectly manufactured VG rotating slowly about a symmetry axis. To graphically analyse our results we transform from fast to slow variables (principal amplitude, quadrature amplitude, precession angle and phase angle variables). We conduct a numerical experiment on the transformed equations of motion that visually demonstrates that anisotropic quadratic nonlinear damping produces principal and quadrature vibrations that are damped down at different rates (as expected). The experiment indicates that the precession rate varies with time, in contrast to the constant precession rate stipulated by Bryan's law for an ideal VG. This evidence suggests that control mechanisms should be investigated in future that will minimise or eliminate anisotropic damping effects that may be present in VGs.

Bryan's factor; vibratory gyroscope; anisotropic nonlinear damping

1. Introduction

With regard to G.H. Bryan's publication [1] in 1890, we call the following Bryan's law (or Bryan's effect)

> *The vibration pattern of a revolving cylinder or bell revolves at a rate proportional to the inertial rotation rate of the cylinder or bell.*

Vibratory gyroscopes (VGs) exploit this law. Indeed, a vibratory gyroscope (VG) operates using Bryan's effect and Bryan's factor (the proportionality constant mentioned in the law).

Linear and nonlinear isotropic damping **does not** affect Bryan' law in a VG as demonstrated in [2]. It is well-known that a frequency split affects Bryan's law (see for instance [3]). We show in this paper that even if no frequency split is present in the VG *any form of anisotropic damping* does affect Bryan's law and hence VG accuracy.

Notation is discussed in Section 2 while Section 3 discusses a new generalised form of Rayleigh's dissipation function, leading to nonlinear tangentially anisotropic damping. Equations of motion are briefly discussed in Section 4 and a transform from fast to slow variables is conducted in Section 5. Penultimately a numerical experiment is performed on the transformed equations of motion in Section 6 and ultimately some conclusions are drawn in Section 7.

2. Notation

We work in a polar coordinate system $Or\varphi$ and refer the reader to [4] (and in particular Fig. 1) for notation, but we might have considered other curvilinear systems $Or\varphi k$ with k an "axis of symmetry" variable, r a "radial" variable and φ a "tangential" variable.

As discussed in [4] we use the small dimensionless positive parameter ε to indicate the "smallness" of a quantity. For instance by the "*smallness of the inertial (angular) rate of rotation*" about the axis of symmetry $\varepsilon\Omega$, we mean that this rate is *substantially smaller than the lowest eigenvalue* ω_0 of the vibrating system. Consequently $O(\varepsilon^2)$ terms such as centripetal forces (proportional to $\varepsilon^2\Omega^2$) are neglected.

Consider a particle P in the VG under consideration (see for instance Fig. 1 of [4]). Assume that u is "radial", v is "tangential" and w is "axial" displacement with

$$u = U\left[C(t)\cos m\varphi + S(t)\sin m\varphi\right], \tag{1}$$

$$v = V\left[C(t)\sin m\varphi - S(t)\cos m\varphi\right], \tag{2}$$

$$w = W\left[C(t)\cos m\varphi + S(t)\sin m\varphi\right], \tag{3}$$

where m is the *circumferential wave number* U, V and W are *eigenfunctions* of one or two variables appropriate to the coordinate system. The functions $C(t)$ and $S(t)$ are *dimensionless* functions of time and the eigenfunctions have the dimensions of length. In this paper we take $w = 0$ and assume that all unbalanced forces in the axial z-direction are zero. Ultimately, *the equations of gyroscopic motion* for each system under similar constraints will be identical.

For completeness we reproduce the definite integrals $I_{0,}I_{1,}$ I_2 and I_3 given in Eqs. (14), (15), (16) and (17) of [5], which occur in the calculation of the kinetic and potential energy for a disk VG (DVG). For the annular disc in [4] Fig. 1 they are:

$$I_0 = \frac{1}{2}\rho_0 h\int_p^q \left(U^2+V^2\right)rdr,\ I_1 = \rho_0 h\int_p^q UVrdr,\ I_3 = \rho_0 h\int_p^q \left(U^2-V^2\right)rdr, \tag{4}$$

$$I_2 = \frac{Eh}{4\left(1-\mu^2\right)}\int_p^q \frac{1}{r}\left\{\begin{array}{c} 2rU'\left(\mu\left(mV+U\right)+rU'\right)+ \\ \left(1-\mu\right)\left(mU+V-rV'\right)^2+ \\ 2(mV+U)\left(mV+U+\mu rU'\right)\end{array}\right\}dr, \tag{5}$$

where E is Young's modulus of elasticity, μ is Poisson's ratio (see, e.g., [6]), ρ_0 is average mass density and h is the height of the disc.

It was demonstrated in [7] (for the appropriate definite integrals of the spherical VG studied there), that Bryan's factor η and the *ideal* VG natural angular rate or eigenvalue $\omega = 2\pi f$ (where f is the natural frequency or eigenfrequency of vibration) are given respectively by

$$\eta = \frac{I_1}{I_0} \quad \& \quad \omega^2 = \frac{I_2}{I_0}. \tag{6}$$

3. Generalised Rayleigh dissipation

In order to introduce nonlinear damping into the equations of motion, we first consider Rayleigh's dissipation function $\mathcal{R}$ (discussed by Lord Rayleigh [8] in Section 81 and, for example, Goldstein

et al. [9], Section 1.5) by adapting Eq. (11) of [10] to represent damping within the volume V of the structure under consideration. If there are various layers in the structure, then we would possibly take a sum of integrals, one for each layer. Analogous to [2] Eq. (8), in order to introduce *nonlinear damping,* for $n = 1, 2, 3, \cdots$ we consider a sequence of dissipation functions

$$\mathcal{R}_n = \frac{1}{2}\int_V \Delta_n(\varphi)\left(\dot{u}^2 + \dot{v}^2 + \dot{w}^2\right))dV; \quad n = 1, 2, 3, \cdots. \tag{7}$$

where only finitely many of the $\mathcal{R}_n \neq 0$. For example, setting $\mathcal{R}_{n>2} = 0$ models a combination *of linear and quadratic* damping (see [2] Fig. 3 for the isotropic case). Defining the generalised Rayleigh dissipation function

$$R = \sum_{n=1}^{\infty} \frac{2}{(n+1)}\left(\sqrt{\mathcal{R}_n}\right)^{n+1} \tag{8}$$

and, considering a Fourier series for the periodic *damping coefficients* $\Delta_n(\varphi)$, we obtain

$$R = \varepsilon\pi I_0 \sum_{n=1}^{\infty} \frac{2}{n+1}\frac{\left(\sqrt{\delta_n}\right)^{n+1}}{\omega^{n-1}}. \tag{9}$$

In Eq. (9) we have

$$\delta_n(\dot{C}, \dot{S}) = \delta_{0,n}^{\frac{2}{n+1}}(\dot{C}^2 + \dot{S}^2) + \tilde{\varepsilon}(\hat{c}_n\, \delta_{c,n}^{\frac{2}{n+1}}(\dot{C}^2 - \dot{S}^2) + 2\hat{s}_n\, \delta_{s,n}^{\frac{2}{n+1}}\dot{C}\dot{S}) \tag{10}$$

with $\delta_{0,n} > 0$ being the "isotropic damping" coefficient that is proportional to the zeroth harmonic of the Fourier series, $\delta_{c,n} > 0$ (respectively $\delta_{s,n} > 0$) being the "anisotropic damping coefficient" proportional to the cosine (respectively sine) $2m^{th}$ harmonic of the Fourier series, with $\hat{c}_n$ (respectively $\hat{s}_n$) being the sign of the cosine (respectively sine) $2m^{th}$ harmonic of the Fourier series and ω being the angular frequency of the mode of vibration m under consideration. The small quantity ε reminds us that damping is light, while the small quantity $\tilde{\varepsilon} > 0$ reminds us that the anisotropic part of the damping is small enough so that $\delta_n(\dot{C}, \dot{S}) > 0$. Keeping the Euler-Lagrange equations in mind (see [2]) it is readily seen that

$$\frac{\partial R}{\partial \dot{C}} = 2\pi I_0 \varepsilon \sum_{n=1}^{\infty}\left(\frac{\sqrt{\delta_n}}{\omega}\right)^{n-1}\left[\left(\delta_{0,n}^{\frac{2}{n+1}} + \tilde{\varepsilon}\hat{c}_n\delta_{c,n}^{\frac{2}{n+1}}\right)\dot{C} + \tilde{\varepsilon}\hat{s}_n\delta_{s,n}^{\frac{2}{n+1}}\dot{S}\right], \tag{11}$$

$$\frac{\partial R}{\partial \dot{S}} = 2\pi I_0 \varepsilon \sum_{n=1}^{\infty}\left(\frac{\sqrt{\delta_n}}{\omega}\right)^{n-1}\left[\left(\delta_{0,n}^{\frac{2}{n+1}} - \tilde{\varepsilon}\hat{c}_n\delta_{c,n}^{\frac{2}{n+1}}\right)\dot{S} + \tilde{\varepsilon}\hat{s}_n\delta_{s,n}^{\frac{2}{n+1}}\dot{C}\right]. \tag{12}$$

4. Equations of motion

As mentioned in the abstract, a VG operates using Bryan's effect. However, Bryan's effect is affected by manufacturing imperfections in mass, stiffness and symmetry. A frequency split in a VG indicates the presence of such imperfections. How to eliminate the frequency split caused by mass and stiffness imperfections was discussed in [4] while an optimal mass-balancing scheme was discussed in [3]. On the other hand, numerous numerical experiments using FEM have been applied similarly in, for example, [11], [12], [13] and [14]. We will assume that frequency split has been eliminated and model an ideal VG where only anisotropic nonlinear damping is introduced into the equations of motion.

Using Eq. (6) of [2], the Lagrangian L of an of the ideal conservative system (where there are no mass-stiffness or symmetry variations within the VG) is given by

$$L(C, \dot{C}, S, \dot{S}) = \pi[I_0(\dot{C}^2 + \dot{S}^2) - 2\varepsilon\Omega I_1(C\dot{S} - \dot{C}S) - (C^2 + S^2)I_2] \tag{13}$$

where definite integrals $I_j; j = 0, 1, 2$ are given in Eqs. (4) and (5) for a DVG.

Keeping Eqs. (6) in mind, substituting Eq. (13) into the Euler-Lagrange equations (see [2]) we obtain

$$\ddot{C} + \omega^2 C = \varepsilon f_1(\dot{C}, \dot{S}), \tag{14}$$

$$\ddot{S} + \omega^2 S = \varepsilon f_2(\dot{C}, \dot{S}). \tag{15}$$

where

$$f_1 = -2\eta\Omega\dot{S} - \frac{1}{2\pi I_0 \varepsilon}\frac{\partial R}{\partial \dot{C}}, \tag{16}$$

$$f_2 = 2\eta\Omega\dot{C} - \frac{1}{2\pi I_0 \varepsilon}\frac{\partial R}{\partial \dot{S}}. \tag{17}$$

These equations of motion could be solved numerically using the formulae for damping given by Eqs. (11) and (12) in order to obtain graphics similar to Figs. 2 and 3 of [2], but we will gain little insight into the affect that nonlinear anisotropic damping has on Bryan's law and hence on VG dynamics. Consequently we transform from fast to slow variables.

5. Principal and quadrature vibration

.

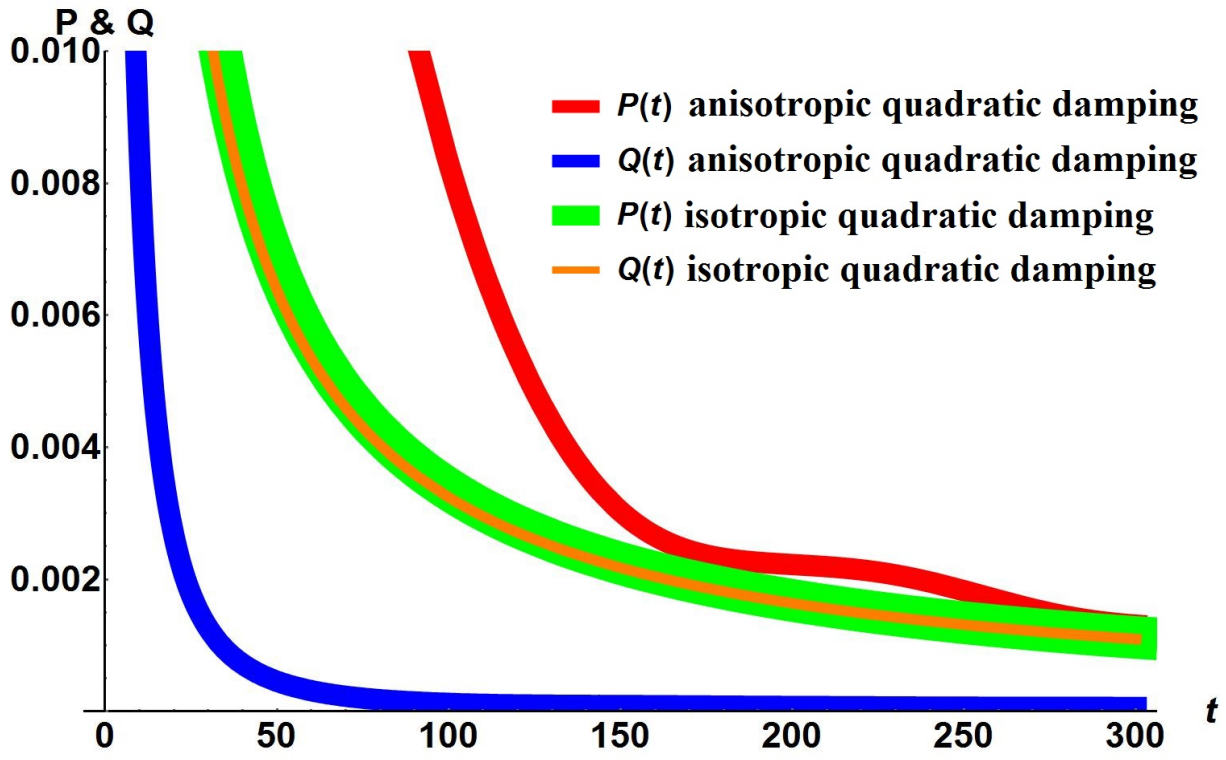

Figure 1: The green and orange curves illustrate that the *isotropic quadratic* damping rate appears to be the same for the amplitudes of the principal P and quadratic Q vibrations. However, the damping rate in the *anisotropic* case is clearly different as illustrated by the red and blue curves.

We introduce a change from "fast" to "slow" variables

$$\Big(C(t), S(t), \dot{C}(t), \dot{S}(t)\Big) \longrightarrow (P(t), Q(t), \Theta(t), \psi(t)) \tag{18}$$

using the transformation

$$C\cos m\varphi + S\sin m\varphi = P\cos[m(\varphi-\Theta)]\cos\gamma + Q\sin[m(\varphi-\Theta)]\sin\gamma \tag{19}$$

where P is the amplitude of the *principal vibration*, Q is the amplitude of the *quadrature vibration*, $m\Theta$ is the *precession angle* (the rotation angle of the vibrating pattern) and ψ is a *phase angle* with

$$\dot{P} = -\frac{\varepsilon}{\omega}[f_1\cos m\Theta + f_2\sin m\Theta]\sin\gamma, \tag{20}$$

$$\dot{Q} = -\frac{\varepsilon}{\omega}[f_1\sin m\Theta - f_2\cos m\Theta]\cos\gamma, \tag{21}$$

$$m\dot{\Theta} = \frac{\varepsilon}{\omega\,(P^2-Q^2)}\{f_1[P\sin m\Theta\sin\gamma + Q\cos m\Theta\cos\gamma] - f_2[P\cos m\Theta\sin\gamma - Q\sin m\Theta\cos\gamma]\}, \tag{22}$$

$$\dot{\psi} = -\frac{\varepsilon}{\omega\,(P^2-Q^2)}\{f_1[P\cos m\Theta\cos\gamma + Q\sin m\Theta\sin\gamma] + f_2[P\sin m\Theta\cos\gamma - Q\cos m\Theta\sin\gamma]\}, \tag{23}$$

where Eqs. (16) and (17) have been transformed according to [15] Eqs. (36) and (40).

6. Numerical experiment

It is well know that in the ideal case, the amplitudes $P(t)$ and $Q(t)$ of the principal and quadrature vibrations (respectively) as well as the phase angle $\psi(t)$ remain constant at the initial values, while the precession angle $m\Theta(t)$ increases linearly from the initial value at a constant rate $\eta\varepsilon\Omega$ where $\varepsilon\Omega$ is the slow inertial rotation rate of the VG and η is Bryan's factor for the VG (see Eq. (6)).

Before conducting numerical experiments using Eqs. (20) through (23)), we need to determine reasonable estimates for quantities in Eqs. (16) and (17) as well as reasonable initial conditions. To achieve this we use the "ideal" aluminium disc described in [16] with inner radius 1.45m and outer radius 1.5m, that at the $m=2$ vibration mode has a natural angular frequency of approximately $\omega_m = 30\pi$rad.s^{-1} and Bryan's factor $\eta_m = -\frac{8}{10}$. We use *anisotropic quadratic* damping ($\delta_{0,n\neq 2} = \delta_{c,n\neq 2} = \delta_{s,n\neq 2} = 0$) in Eqs. (16) and (17). We consider the following values in order to *highlight the influence* of the *anisotropic quadratic damping*:

$$\begin{gathered} m=2, \varepsilon=\tfrac{1}{100}, \tilde{\varepsilon}=\tfrac{1}{10}, \eta_m=-\tfrac{8}{10}, \Omega=\pi rad.s^{-1}, \omega_m=30\pi rad.s^{-1}, \\ n=2, \hat{c}_n=1, \hat{s}_n=-1, \delta_{0,n}=600Hz, \delta_{c,n}=3000Hz, \delta_{c,n}=7500Hz, \\ P(0)=\tfrac{1}{2}, Q(0)=\tfrac{1}{3}, m\Theta(0)=0rad, \psi(0)=0rad, 0\leq t\leq 300s. \end{gathered} \tag{24}$$

It is clear from Fig. 1 that for the anisotropic quadratic case, the damping rate for the amplitude P of the principal vibration is not the same the damping rate of the amplitude of the quadrature vibration Q. This is in sharp contrast to the evidently equal damping rates for the isotropic case.

In [2] it was demonstrated analytically that isotropic nonlinear damping of any order (even combinations of such damping) does not affect the ideal precession rate of a VG and that the precession rate is exactly the same as for the ideal case discussed above, namely $m\dot{\Theta} = \eta\varepsilon\Omega$. Fig. 2 confirms this observation for isotropic quadratic damping and also indicates that the precession rate $m\dot{\Theta}$ is *not a constant* for the anisotropic case. Consequently the presence of such anisotropic damping will severely affect the accuracy of the VG and so it is imperative that control mechanisms for such damping be investigated.

Finally, the numerical experiment indicates that the phase angle $\psi(t)$ deviates from the ideal case for both the anisotropic and isotropic quadratic damping cases although the deviation for anisotropic

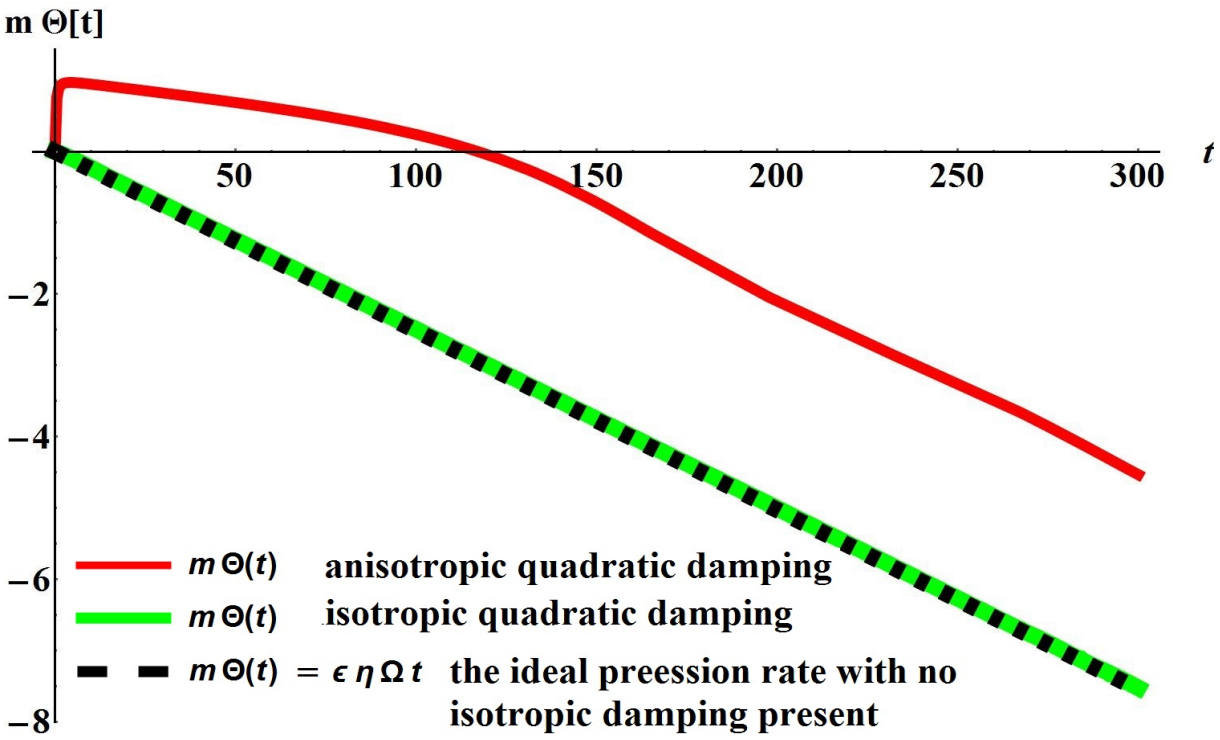

Figure 2: The green straight line represents a numerical solution for the precession angle of the VG when *isotropic quadratic* damping is present . The black dotted straight line superimposed on the green line represents the ideal precession angle of the VG, confirming known results about isotropic damping of any order or combinations of orders. However, the red curve indicates that the presence of *anisotropic quadratic* damping severely affects the precession rate $m\dot{\Theta}$ of the VG and hence the accuracy of the VG.

damping appears to be more drastic than that of the isotropic case. The graph of this situation is shown in Fig. 3.

We have conducted numerical experiments with other vibration modes $m = 3, 4, 5, 6$ and anisotropic damping of orders 3 and 4 and combinations of these types of damping. All experiments return similar results to the anisotropic quadratic case.

7. Conclusion

We have defined a new generalised form of Rayleigh's dissipation function for both isotropic and anisotropic damping of any order or combinations of orders. We have shown how to introduce such damping into the equations of motion of a VG revolving slowly about a symmetry axis. We introduced a numerical experiment that demonstrates that the precession rate of the VG deviates from a constant rate when anisotropic quadratic (and higher order) damping is present.

In future work we will attempt to analyse the transformed equations of motion (Eqs. (20) through (23)) using an "averaging" method (see [15]) that will confirm analytically (up to an average, for any vibration mode m and any combination of any order of damping) the numerical results given above. Furthermore, the numerical results above indicate that it is imperative that control methods be established that limit the effects of ever present damping no matter what form it takes.

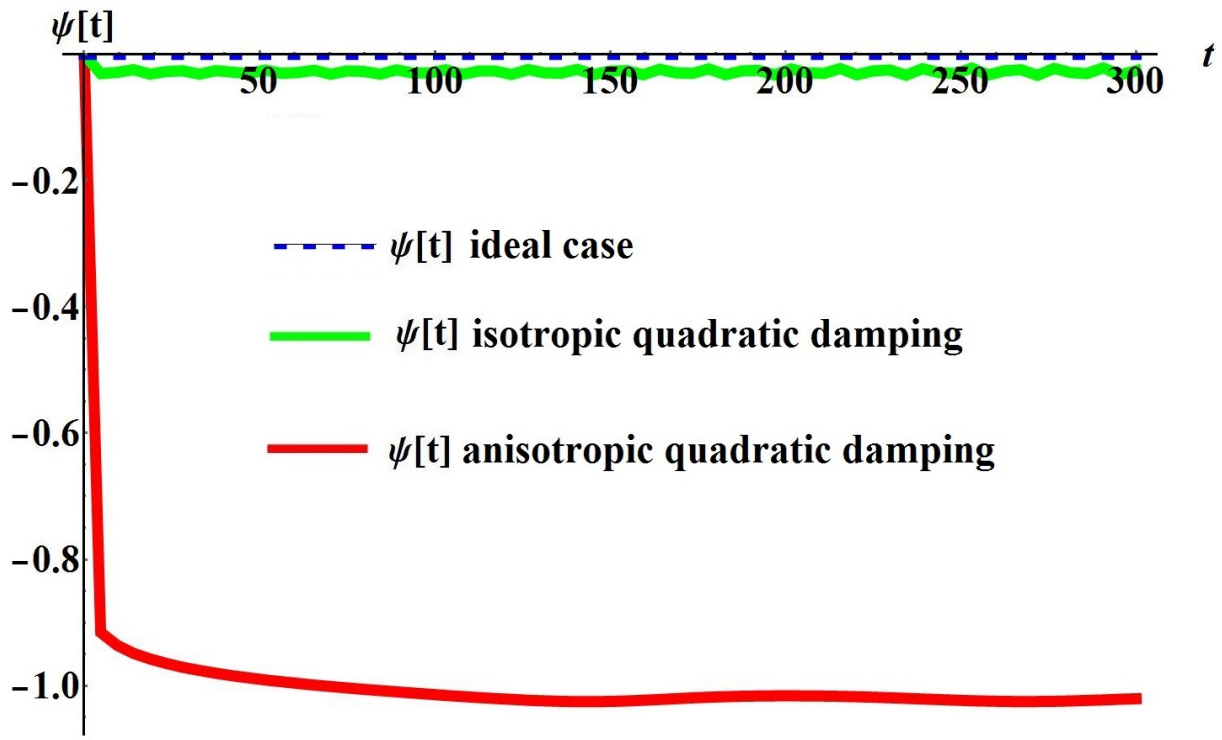

Figure 3: The green curve indicates that *isotropic quadratic* damping has a minimal effect on the phase angle $\psi(t)$, in sharp contrast to the red curve representing the anisotropic case.

8. Acknowledgment

This material is based upon work supported financially by the Tshwane University of Technology (TUT) and the National Research Foundation (NRF) of South Africa (NRF grant reference number IFR160211157784). Any opinions, findings and conclusions or recommendations expressed in this material are those of the authors, and TUT and the NRF therefore do not accept any liability in regard thereto.

REFERENCES

1. Bryan, G. H. On the beats in the vibrations of a revolving cylinder or bell, *Proc Camb Philos Soc Math Phys Sci*, **7**, 101–114, (1890).

2. Joubert, S. V., Shatalov, M. Y. and Manzhirov, A. V. Bryan's effect and isotropic nonlinear damping, *J Sound Vib*, **332**, 6169–6176, (2013).

3. Shatalov, M. Y., Joubert, S. V. and Spoelstra, H. Optimisation of vibratory gyroscopes mass-balancing procedures, *International conference on sound and vibration (ICSV22), Florence, Italy*, pp. 1–8, (2015).

4. Joubert, S. V., Shatalov, M. Y. and Spoelstra, H. Modelling and controlling imperfections in vibratory gyroscopes, *International conference on sound and vibration (ICSV22), Florence, Italy*, pp. 1–8, (2015).

5. Joubert, S. V., Shatalov, M. Y. and Coetzee, C. E. Using Fourier series to analyse mass imperfections in vibratory gyroscopes, *J Symb Comput*, **61-62**, 116–127, (2014).

6. Redwood, M., *Mechanical waveguides*, Pergamon Press, Oxford (1960).

7. Shatalov, M. Y., Joubert, S. V., Coetzee, C. E. and Fedotov, I. Free vibration of rotating hollow spheres containing acoustic media, *J Sound Vib*, **322** (4-5), 1038–1047, (2009).

8. Rayleigh, J. W. S., *The theory of sound, second edition*, MacMillan & Company, London (1894).

9. Goldstein, H., Poole, C. and Safko, J., *Classical Mechanics, third edition*, Addison–Wesley, Reading, MA (2001).

10. Joubert, S. V., Shatalov, M. Y. and Coetzee, C. E. Analysing manufacturing imperfections in a spherical vibratory gyroscope, *4th IEEE International Workshop on Advances in Sensors and Interfaces (IWASI)*, pp. 165–170, (2011).

11. Liu, N., Su, Z., Li, Q., Fu, M., Liu, H. and Fan, J. Characterization of the bell-shaped vibratory angular rate gyro, *Sensors*, **13**, 10123–10150, (2013).

12. Lin, Z., Fu, M., Deng, Z., Liu, N. and Liu, H. Frequency split elimination method for a solid-state vibratory angular rate gyro with an imperfect axisymmetric shell-resonator, *Sensors*, **15**, 3204 – 3223, (2015).

13. Wang, Y., Wang, S. and Zhu, D. Dual-mode frequency splitting elimination of ring periodic structures via feature shifting, *J. Mech. Eng. Sci.*, **203–210**, 1989–1996, (2015).

14. Liu, N., Su, Z. and Li, Q. Design and experiment of a novel bell-shaped vibratory gyro, *Sensors and Actuators A: Physical*, **238**, 37–50, (2016).

15. Shatalov, M. Y., Joubert, S. V. and Coetzee, C. E. The influence of mass imperfections on the evolution of standing waves in slowly rotating spherical bodies, *J Sound Vib*, **330**, 127–135, (2011).

16. Joubert, S. V., Shatalov, M. Y. and Fay, T. H. On numerically solving an eigenvalue problem arising in a resonator gyroscope, *Appl Math and Comput*, **246**, 561–571, (2014).